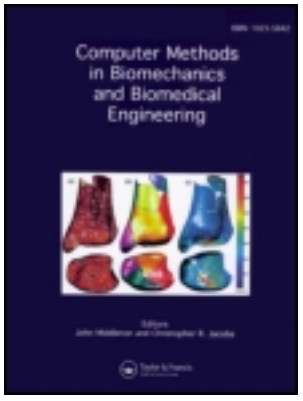

Computer Methods in Biomechanics and Biomedical Engineering
Publication details, including instructions for authors and subscription information:
http://www.tandfonline.com/loi/gcmb20

The influence of different magnitudes and methods of applying preload on fusion and disc replacement constructs in the lumbar spine: a finite element analysis

Zheng-Cheng Zhong[a], Chinghua Hung[b], Hung-Ming Lin[c], Ying-Hui Wang[a], Chang-Hung Huang[d] & Chen-Sheng Chen[a]

[a] Department of Physical Therapy and Assistive Technology, National Yang-Ming University, 155, Section 2, Li-Nung Street, Taipei, Taiwan

[b] Department of Mechanical Engineering, National Chiao-Tung University, Hsinchu, Taiwan

[c] Department of Mechanical Engineering, National Taiwan University, Taipei, Taiwan

[d] Department of Biomedical Research, Mackay Memorial Hospital, Tamshui, Taipei County, Taiwan

Published online: 06 Jan 2012.

To cite this article: Zheng-Cheng Zhong, Chinghua Hung, Hung-Ming Lin, Ying-Hui Wang, Chang-Hung Huang & Chen-Sheng Chen (2013) The influence of different magnitudes and methods of applying preload on fusion and disc replacement constructs in the lumbar spine: a finite element analysis, Computer Methods in Biomechanics and Biomedical Engineering, 16:9, 943-953, DOI: 10.1080/10255842.2011.645226

To link to this article: http://dx.doi.org/10.1080/10255842.2011.645226

Computer Methods in Biomechanics and Biomedical Engineering, 2013
Vol. 16, No. 9, 943–953, http://dx.doi.org/10.1080/10255842.2011.645226

Taylor & Francis
Taylor & Francis Group

The influence of different magnitudes and methods of applying preload on fusion and disc replacement constructs in the lumbar spine: a finite element analysis

Zheng-Cheng Zhong[a], Chinghua Hung[b], Hung-Ming Lin[c], Ying-Hui Wang[a], Chang-Hung Huang[d] and Chen-Sheng Chen[a]*

[a]*Department of Physical Therapy and Assistive Technology, National Yang-Ming University, 155, Section 2, Li-Nung Street, Taipei, Taiwan;* [b]*Department of Mechanical Engineering, National Chiao-Tung University, Hsinchu, Taiwan;* [c]*Department of Mechanical Engineering, National Taiwan University, Taipei, Taiwan;* [d]*Department of Biomedical Research, Mackay Memorial Hospital, Tamshui, Taipei County, Taiwan*

(*Received 25 March 2011; final version received 27 November 2011*)

In a finite element (FE) analysis of the lumbar spine, different preload application methods that are used in biomechanical studies may yield diverging results. To investigate how the biomechanical behaviour of a spinal implant is affected by the method of applying the preload, hybrid-controlled FE analysis was used to evaluate the biomechanical behaviour of the lumbar spine under different preload application methods. The FE models of anterior lumbar interbody fusion (ALIF) and artificial disc replacement (ADR) were tested under three different loading conditions: a 150 N pressure preload (PP) and 150 and 400 N follower loads (FLs). This study analysed the resulting range of motion (ROM), facet contact force (FCF), inlay contact pressure (ICP) and stress distribution of adjacent discs. The FE results indicated that the ROM of both surgical constructs was related to the preload application method and magnitude; differences in the ROM were within 7% for the ALIF model and 32% for the ADR model. Following the application of the FL and after increasing the FL magnitude, the FCF of the ADR model gradually increased, reaching 45% at the implanted level in torsion. The maximum ICP gradually decreased by 34.1% in torsion and 28.4% in lateral bending. This study concluded that the preload magnitude and application method affect the biomechanical behaviour of the lumbar spine. For the ADR, remarkable alteration was observed while increasing the FL magnitude, particularly in the ROM, FCF and ICP. However, for the ALIF, PP and FL methods had no remarkable alteration in terms of ROM and adjacent disc stress.

Keywords: lumbar spine; preload; follower load; finite element method; spinal fusion; total disc replacement

Introduction

The human lumbar spine can withstand a compressive load up to 2.5 times the body weight during walking (Cappozzo 1984). However, it is difficult to mimic this condition in long specimens of the lumbar spine in *in vitro* experimental studies because the spine is unstable under a very low vertical compressive preload (Yamamoto et al. 1989; Crisco et al. 1992). Because of the curvature of the lumbar spine, this load causes bending moments and shear forces when applied at the superior end of the specimen (Patwardhan et al. 1999). In addition, spine specimens in *in vitro* tests are unsupported by local muscle activation, which results in a lower load-carrying capacity than in the *in vivo* condition.

Patwardhan et al. (1999) proposed a 'follower load' (FL) preload technique, in which a compressive preload is applied at the geometric centres of the vertebral bodies along a path that follows the curvature of the lumbar spine. Several studies have demonstrated that an FL can increase the load-carrying capacity of the intact lumbar spine without damage by gradually changing the load–displacement response from a nonlinear to a linear curve as the FL magnitude increases and by increasing the stiffness of the spine as the compressive FL increases (Patwardhan et al. 1999, 2003b; Rohlmann et al. 2001; Renner et al. 2007). Rohlmann et al. (2009a, 2009b) evaluated various loading modes for simulating upper body bending and the standing posture of the intact lumbar spine and compared these results with data measured *in vivo*. These authors found that applying an FL agrees well with *in vivo* data from the literature. In addition, the role of the trunk muscles in generating an FL in the lumbar spine has been identified by mathematical models; both the frontal- and the sagittal-plane models have shown that trunk muscles can generate an FL *in vivo* (Patwardhan et al. 2001; Kim et al. 2007; Kim and Kim 2008).

The effects of the FL for various lumbar spinal implant constructs were investigated in several studies (Patwardhan et al. 2003b; Phillips et al. 2004; Tzermiadianos et al. 2008). The magnitude of the FL preload significantly affected the range of motion (ROM) of the anterior lumbar interbody fusion (ALIF) cage alone; the cages provided less ROM at a larger FL than at a smaller FL (Patwardhan et al. 2003b). Supplemental translaminar facet screw fixation did not significantly increase the ROM of the ALIF cages in flexion or extension at high preload magnitudes (Tzermiadianos

*Corresponding author. Email: cschen@ym.edu.tw

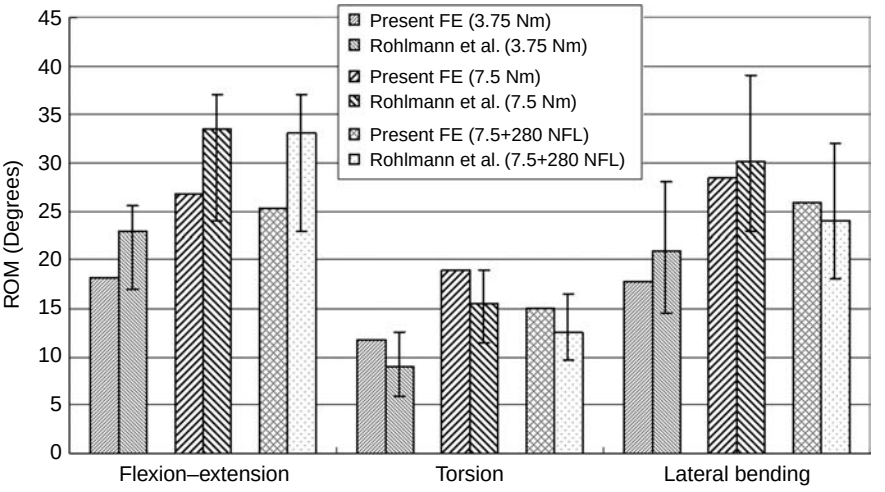

Figure 1. Comparison of the ROM calculated for five levels of the intact lumbar spine with Rohlmann's *in vitro* model. Loading with pure moments of 3.75 and 7.5 Nm with or without an FL of 280 N was applied in each physiological motion. (The data include bilateral ROMs. Median and extreme values for the *in vitro* data are shown.)

et al. 2008). Tzermiadianos et al. (2008) assessed the stabilisation effect of three different instrumentation systems under or without compressive FL. The authors found that an anterior tension band plate exhibited a significantly smaller flexion–extension ROM under physiological compressive FL than without FL. O'Leary et al. (2005) evaluated prosthesis component motion patterns of the Charité total disc replacement system under or without physiological FL. They found that the prosthesis component motion patterns were altered and that the flexion–extension ROM was restored to near-normal levels under a physiological FL.

Different magnitudes and methods of applying preload used in biomechanical studies may yield divergent findings. However, little is known about the effects of the different preload application methods or magnitudes on the implant and the surrounding tissues. Therefore, the purpose of this study was to investigate the influence of the preload application method and magnitude on ALIF and artificial disc replacement (ADR) constructs with respect to the ROM, facet contact force (FCF), inlay contact pressure (ICP) of the disc arthroplasty and stress distribution of the L2/L3 disc annulus.

Materials and methods

FE model of the intact lumbar spine (INT model)

The geometry of a three-dimensional (3D) L1–L5 intact (INT) lumbar spine finite element (FE) model was acquired from computed tomography images and built using the FE analysis software (ANSYS 11.0, ANSYS Inc., Canonsburg, PA, USA). The INT model includes the vertebrae, intervertebral discs, endplates, posterior bony elements and all seven ligaments (the anterior and posterior longitudinal ligaments, ligamentum flavum, facet capsules, and the intertransverse, interspinous and supraspinous ligaments).

The cortical bone, cancellous bone, endplate, posterior bony element and annulus ground substance were modelled by an eight-node continuum element type (SOLID 185). The cortical and cancellous bone was modelled based on orthotropic material properties, which can describe the ability to resist larger vertebral vertical compressive loads. For the disc, 12 double cross-linked fibre layers were embedded in the ground substance and defined to decrease the elastic modulus and cross-sectional area proportionally from the outermost layer to the innermost layer (Shirazi-Adl et al. 1986). The ground substance was simulated by a hyperelastic Mooney–Rivlin material model. Of the cross-sectional area in the disc, 43% was defined as the nucleus, which is within the range of 30–50% reported by Panagiotacopulos et al. (1987). The nucleus pulposus was modelled by an eight-node fluid element as an incompressible fluid with a bulk modulus of 1666.7 MPa (Lu et al. 1996). All seven ligaments were simulated by a two-node truss element (LINK 10) with uniaxial tension resistance-only behaviour. The facet joint surfaces were treated as having sliding contact behaviour, using an eight-node surface-to-surface contact element, and the coefficient of friction used was 0.1 (Polikeit et al. 2003). A more detailed description of the material properties of the spine FE model can be found in our previous studies (Chen et al. 2009; Zhong et al. 2009).

Convergence test and model validation

For the convergence test, the loading condition of the test was 10 Nm moment, and a 150 N preload acted on the

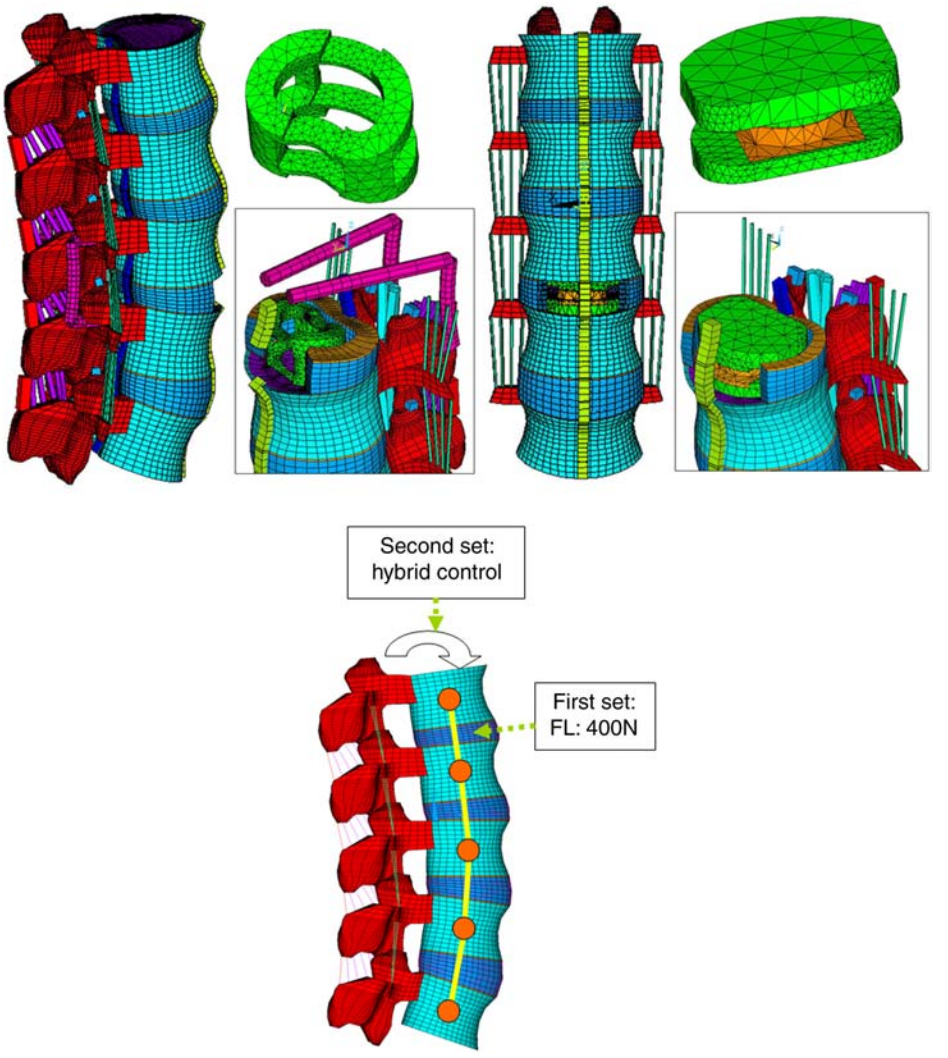

Figure 2. FE model of the L1–L5 segments after ALIF with a SynCage combined with posterior pedicle screw fixation at L3/L4 (top, left) or total disc replacement with a ProDisc II artificial disc at L3/L4 (top, right). Two loading sets of the FE model (bottom).

superior surface of the L1 vertebra. Three mesh densities (coarse model: 4750 elements/4960 nodes; normal model: 27,244 elements/30,630 nodes; finest model: 112,174 elements/94,162 nodes) were selected to test ROM changes in the INT model, and the finest mesh density was selected because the changes between the normal model and finest model were within 1.03% in flexion (less than 0.2°), 4.39% in extension (less than 0.5°), 0.01% in torsion (less than 0.2°) and 0.001% in lateral bending (less than 0.1°; Liu et al. 2011). The element size was approximately 2.5 mm.

The spine model has been validated by comparing the five-level lumbar ROMs under different magnitudes of pure moment against values from the previous literature; this comparison was described in our earlier studies (Zhong et al. 2009). In addition, this study applied pure moments of 7.5 Nm with or without a 280 N FL to validate

Table 1. The material properties used in an FE model of spinal implants.

Material	Element type	Young's modulus (MPa)	Poisson's ratio
Fusion construct			
Spinal instrumentation system (titanium alloy)	2-node BEAM188	110,000	0.28
SynCage-Open (titanium alloy)	8-node SOLID185	110,000	0.28
Disc arthroplasty construct			
ProDisc II metallic endplate (Co–Cr–Mo alloy)	8-node SOLID185	210,000	0.30
ProDisc II inlay (Ultra-high molecular weight polyethylene)	8-node SOLID185	1016	0.46

Table 2. Intervertebral ROM (degrees) and applied moment (Nm) for the INT, ALIF and ADR models under three different compressive preloads.

	L2/L3 (upper adjacent level)	L3/L4 (implanted level)	L4/L5 (lower adjacent level)	Total lumbar ROM (L1–L5)	Moment (Nm)
Flexion					
INT-150PP	3.93	4.00	5.15	16.84	10.0
ALIF-150PP	4.92	0.65	6.55	16.81	12.9
ADR-150PP	3.76	4.25	5.08	16.74	9.6
INT-150FL	3.89	3.94	5.15	16.74	10.0
ALIF-150FL	4.87	0.65	6.63	16.81	12.9
ADR-150FL	3.86	3.84	5.22	16.69	9.6
INT-400FL	3.83	3.86	5.09	16.51	10.0
ALIF-400FL	4.74	0.62	6.63	16.53	12.9
ADR-400FL	3.95	3.32	5.32	16.47	10.0
Extension					
INT-150PP	3.37	3.70	4.36	14.73	10.0
ALIF-150PP	4.24	0.65	5.55	14.82	16.2
ADR-150PP	2.91	5.36	3.64	14.86	6.9
INT-150FL	3.12	3.44	4.08	13.79	10.0
ALIF-150FL	3.93	0.49	5.28	13.85	15.9
ADR-150FL	2.89	4.24	3.69	13.71	7.5
INT-400FL	2.81	3.14	3.71	12.61	10.0
ALIF-400FL	3.59	0.30	4.92	12.70	15.6
ADR-400FL	2.62	4.08	3.44	12.76	7.8
Torsion					
INT-150PP	2.16	2.50	2.79	9.48	10.0
ALIF-150PP	2.46	1.31	3.20	9.43	13.2
ADR-150PP	1.85	3.56	2.37	9.50	7.8
INT-150FL	2.06	2.40	2.67	9.08	10.0
ALIF-150FL	2.38	1.14	3.15	9.05	13.2
ADR-150FL	1.89	3.10	2.42	9.18	8.4
INT-400FL	1.94	2.26	2.52	8.57	10.0
ALIF-400FL	2.25	1.03	3.02	8.57	13.2
ADR-400FL	1.84	2.51	2.41	8.53	9.0
Lateral bending					
INT-150PP	4.05	4.25	4.87	17.14	10.0
ALIF-150PP	4.92	1.31	6.02	17.14	12.3
ADR-150PP	3.57	5.82	4.41	17.06	9.0
INT-150FL	3.83	4.00	4.65	16.31	10.0
ALIF-150FL	4.66	1.16	5.89	16.48	12.3
ADR-150FL	3.51	5.20	4.36	16.27	9.0
INT-400FL	3.60	3.68	4.28	15.24	10.0
ALIF-400FL	4.35	1.01	5.53	15.37	12.0
ADR-400FL	3.20	4.61	3.99	15.11	9.0

Notes: INT, intact spine; ALIF, anterior lumbar interbody fusion; ADR, artificial disc replacement; 150PP, pressure preload of 150 N; 150FL, follower load of 150 N; 400FL, follower load of 400 N.

the INT model after the addition of FL. Compared with results of the *in vitro* cadaveric tests of Rohlmann et al. (2001), the ROMs under four physiological motions all fell within similar ranges, and the trends agreed well with their experimental test to determine whether FL increased the stiffness of the INT model (Figure 1).

FE model of the ALIF model

To simulate the ALIF, the L3/L4 level of the INT model underwent partial discectomy and total nuclectomy according to standard surgical procedures, which included the removal of the anterior longitudinal ligament (ALL), anterior portions of the annulus and the entire nucleus pulposus. An 8° lordotic titanium alloy cage (SynCage-Open, Synthes Spine, Inc., Mathys Medical Ltd, Bettlach, Switzerland; 30 mm × 24 mm × 21 mm) that was supplemented with a bilateral pedicle screw fixation device was inserted at the L3/L4 level. The pedicle screws and rods had a diameter of 6 mm and were modelled using 3D beam elements. The bone–screw and bone–cage interfaces were assigned to fully constrained and fully bonded behaviour, respectively, to mimic a successful fusion. Figure 2 (left) shows the ALIF model and remaining tissues after insertion of an anterior cage and fixation system. The material properties of the implant components are listed in Table 1.

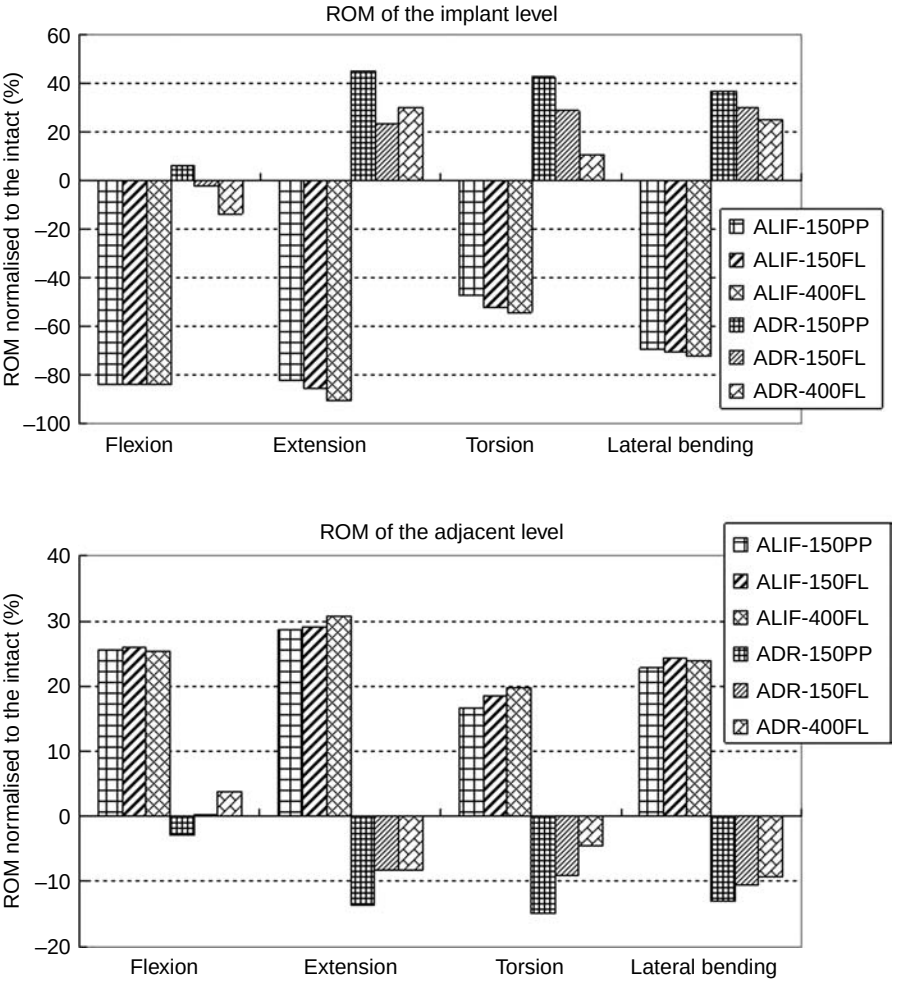

Figure 3. Changes in the ROM (% of intact) at the implanted (top) and adjacent (bottom) levels under flexion, extension, torsion and lateral bending.

FE model of the anterior lumbar ADR model

To simulate the ADR, the anterior portions of the annulus and the entire nucleus at L3/L4 were removed. An artificial disc (ProDisc II, Synthes, Inc., Paoli, PA, USA/Spine Solution, New York, NY, USA) was implanted in the INT model at L3/L4 and was modelled by an eight-node solid element. The ALL was preserved to represent suture closure of the ALL after the insertion of a disc arthroplasty. The keel of the metallic plate surfaces was modelled as a flat surface for simplification. A fully bonded behaviour was applied between the metallic plate and adjacent vertebrae. A ball-and-socket surface was simulated with a deformable 3D surface-to-surface contact element, and the coefficient of friction of 0.07 was used for the polyethylene–Co–Cr–Mo alloy interface (Godest et al. 2002). Figure 1(b) shows the ADR model and the remaining tissues after the ProDisc II was implanted. The material properties of the ProDisc II components are listed in Table 1.

Boundary and loading conditions

All degrees of freedom were constrained at the bottom of the fifth vertebra for all of the FE models. Three different preload loading conditions were used in this study: a pressure preload of 150 N (150PP) and FLs of 150 N (150FL) and 400 N (400FL). The pressure preload (PP) technique calls for applying pressure at the top surface of L1 to create a compressive force of 150 N that is always perpendicular to the superior end of the spinal column. The FL was simulated by a two-node link element that was attached near the geometric centre of each vertebra, and either a 150 N or a 400 N compressive force was produced by contracting the link elements via environmental temperature control (Renner et al. 2007). The elastic modulus of these link elements was low (0.1% of cortical bone), in order to diminish the influence of the stiffness of the link elements. The optimal FL path of each FE model was defined by trial and error by adjusting the attachment

points of the link elements. Finally, the optimised FL paths were able to restrict the ROM of each motion segment to within 0.2°, 0.3° and 0.31° for the INT, ALIF and ADR models, respectively.

In real life, people complete a motion within a limited ROM regardless of whether their spine is healthy or has undergone spinal surgery. Consequently, limited ROM is used to evaluate the biomechanical effect of different spinal surgeries during daily activity. In addition, the main objective of the patient after spinal surgery is to return to normal daily life. Thus, the treated lumbar spine should be able to complete the same ROM that a normal lumbar spine can. A hybrid testing protocol was used in this study and has been described in detail in previous studies (Goel et al. 2005). The INT model was subjected to each of the three different preloads and combined with moments of 10 Nm. The ROMs (L1–L5) of the ALIF and ADR models that were determined for each preload application method, combined with various moments, matched the ROMs of the INT model for each physiological motion; the data for the various moments are shown in Table 2. The deviation in ROM for each of the three FE models was within 0.12° in flexion, 0.15° in extension, 0.10° in torsion and 0.26° in lateral bending (Table 2).

Results

The results included the ROM, FCF and ICP of the disc arthroplasty, the stress distribution of the adjacent L2/L3 disc annulus and the maximum stress of the L3 pedicle screws. All of the ROM and FCF data were normalised to the INT model as percentage values at each loading mode.

Range of motion

For the implanted level, the ALIF model displayed a relatively similar ROM compared with the INT model. Compared with results from the ALF model using the preload method and FL magnitude, the differences were small (within 7%). The ADR model displayed relative mobility compared with the INT model. Under a load of 150 N, the differences between the preload application methods in the ADR model showed that FL reduced the ROM by 22% in extension and by 14% in torsion. Increasing the FL magnitude for the ADR model resulted in a further ROM decrease by 18.2% in torsion (Figure 3, top). The ROM values are shown in Table 2.

For the adjacent level, the ALIF model showed relative mobility (at least a 17% increase in ROM) compared with the INT model. Compared with the ALIF model using the preload method and FL magnitude, the difference was small (within 3%). The ADR model exhibited a relatively high ROM compared with the INT model. The use of FL for the ADR model resulted in the ROM approach to the INT model (Figure 3, bottom).

Table 3. Comparison of FCF among the different FE models (unit: N).

	L2/L3 (adjacent level)	L3/L4 (implanted level)
Extension		
INT-150PP	47	73
ALIF-150PP	117	0
ADR-150PP	30	76
INT-150FL	53	74
ALIF-150FL	121	0
ADR-150FL	33	65
INT-400FL	59	74
ALIF-400FL	126	0
ADR-400FL	32	56
Torsion		
INT-150PP	130	125
ALIF-150PP	178	58
ADR-150PP	101	132
INT-150FL	125	120
ALIF-150FL	176	40
ADR-150FL	107	147
INT-400FL	119	116
ALIF-400FL	170	26
ADR400FL	108	168

Facet contact force

The direction of torsion was counterclockwise. All of the FCFs occurred at the contralateral side (right side). For the implanted level, the ALIF model resulted in no FCF in extension and clearly decreased FCF in torsion (at least 54%) compared with the INT model (Table 3). The use of FL resulted in a further FCF decrease in torsion. The ADR model revealed that FCF was increased in torsion compared with the INT model. The difference between preload application methods for the ADR model showed that FL increased FCF by 17.4% in torsion. Increasing the FL magnitude in the ADR model resulted in a further FCF increase by 22.4% in torsion (Figure 4, top).

For the adjacent level, the ALIF model showed that FCF increased by at least 121% in extension and by 37% in torsion compared with the INT model. Compared with the results from the ALIF model using the preload method and FL magnitude, the differences in torsion were small (within 6%); however, a higher FL clearly decreased the FCF by 27% in extension. The ADR model revealed that the FCF was lower than the INT model in extension and torsion. The use of FL and increasing FL magnitude resulted in the FCF approach to the INT model (Figure 4, bottom).

Stress distribution of the L2/L3 disc annulus

Figure 5 illustrates the stress distribution of the adjacent disc annulus under different preloads among the three FE models (flexion). A higher stress concentration is more clearly shown in the ALIF model (solid arrow), whereas

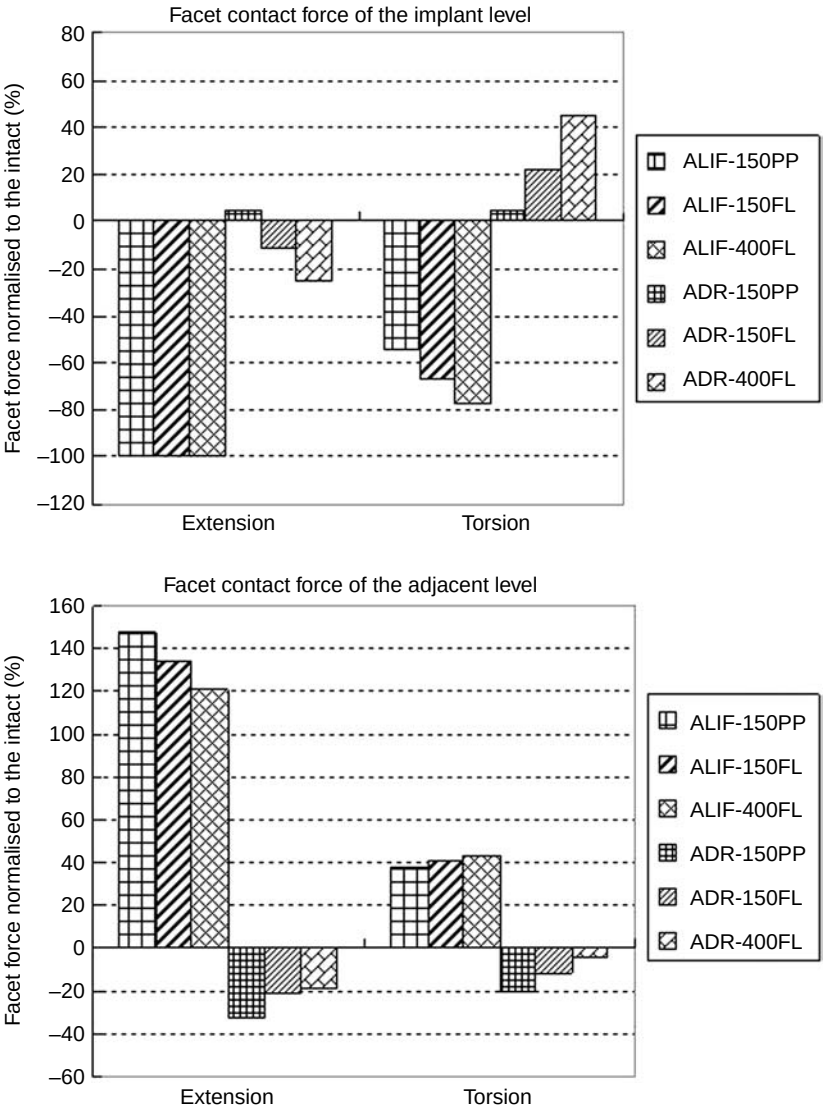

Figure 4. Changes in the FCF (% of intact) at the implanted (top) and adjacent (bottom) levels under extension and torsion.

the stress distribution was similar to that seen in the intact spine in the ADR model, regardless of whether pressure or follower preload was used. The dotted arrows indicate that the annulus stress was concentrated anteriorly and posteriorly under PP; however, the stress distribution pattern changed and was concentrated only at sites of motion (anterior regions) under FL. Similar trends were also found during other physiological motions.

ICP of the disc arthroplasty

The maximum ICP occurred in the ADR-150PP model in torsion and reached 8.15 MPa. The ICP clearly decreased in torsion (34.1%) and in lateral bending (28.4%) under a higher FL of 400 N (Table 4). Figure 6 shows that the contact region gradually increased when FL was used and the FL magnitude rose. In particular, the inlay was observed to be completely unloading in extension, except at a physiological FL of 400 N.

Discussion

An FE model was used to study the effects of different magnitudes and methods of applied preload in ALIF versus ADR constructs on an implant and its surrounding tissues.

Results from the present INT model with FL were in agreement with the *in vitro* tests of Rohlmann et al. (2001), in which the ROM decreased during torsion and lateral bending but did not change during flexion–extension. Therefore, the INT model under FL was validated in this study. Patwardhan et al. (1999) indicated that the lumbar

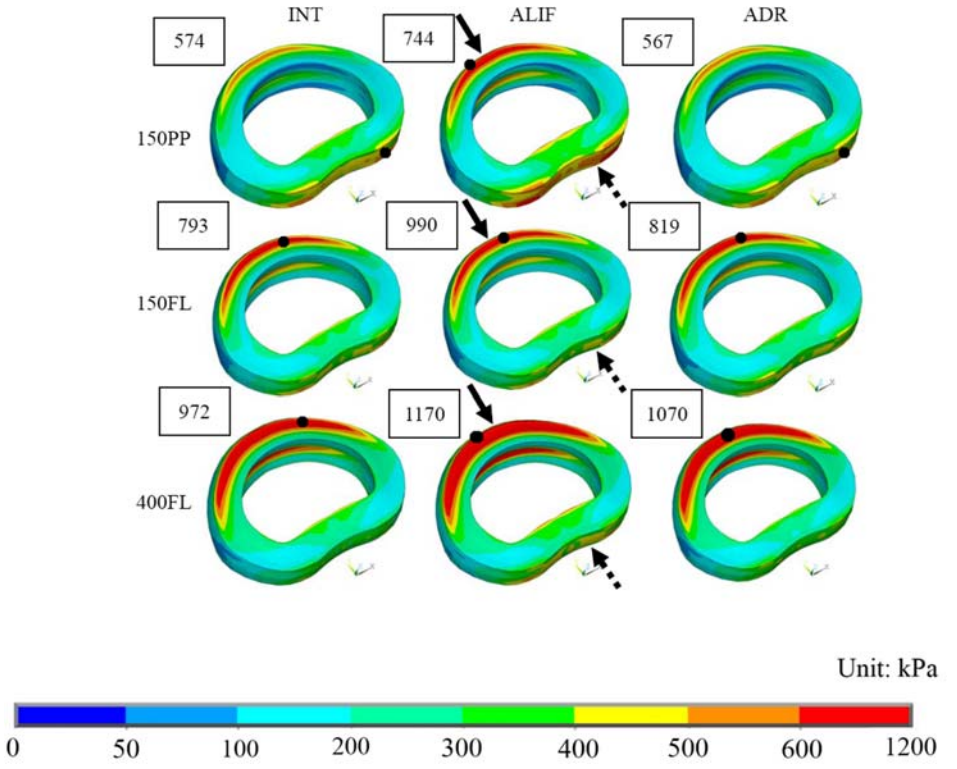

Figure 5. Von Mises stress distribution of the adjacent L2/L3 disc annulus in flexion in the INT model (left), ALIF model, ADR model (right) under a PP of 150 N (top), FL of 150 N and FL of 400 N (bottom). The solid arrows indicate prominently increased stress concentration regions. The dotted arrows show regions of altered stress distribution patterns. The square box indicates the maximum stress value. The black dot indicates the location of the maximum stress.

ROM changed by 10–15° when a small vertical preload of 100 N was applied to L1. However, results from our INT model with a PP were inconsistent with Patwardhan's finding. This conflicting result likely occurred because the PP technique creates a compressive force that is always perpendicular to the superior end of the spinal column when the specimen is deformed under loading, which causes fewer artefactual forces than does the vertical preload technique.

Several *in vitro* studies indicated that increased FL magnitudes increased the stabilisation provided by fusion implants (Patwardhan et al. 2003a; Phillips et al. 2004; Tzermiadianos et al. 2008). This study revealed that the ROM for both of the surgical constructs is related to the preload application method and magnitude; differences in ROM were within 7% for the ALIF model and 32% for the ADR model. In addition, in this study, it was found that the ROM in the total disc replacement case for either the implanted or the adjacent segments was closer to the intact state when physiological FL was used. This result implies that the role of the muscle is more important in stabilising and restoring normal motion in patients who have undergone total disc replacement than for those who have undergone spinal fusion.

Several clinical researchers have reported complications following the implantation of an artificial disc, including facet hypertrophy at the implanted level, when either a ball-and-socket or a mobile core design was used. The rates of degeneration ranged from 11% to 36.4% (van Ooij et al. 2003; Lemaire et al. 2005; Shim et al. 2007).

Table 4. Maximum ICP of the disc arthroplasty under different preload methods.

		Physiological motion		
FE model	Flexion	Extension	Torsion	Lateral bending
ADR-150PP	4.18	Lift-off	8.15	6.97
ADR-150FL	4.44 (+6.2%)	Lift-off	7.86 (−3.6%)	4.86 (−30.3%)
ADR-400FL	5.23 (+25.1%)	3.29	5.00 (−34.1%)	4.99 (−28.4%)

Notes: ADR, artificial disc replacement; 150PP, pressure preload of 150 N; 150FL, follower load of 150 N; 400FL, follower load of 400 N. The data inside the parentheses are ICP normalised to the ADR-150PP model for each motion (units: MPa).

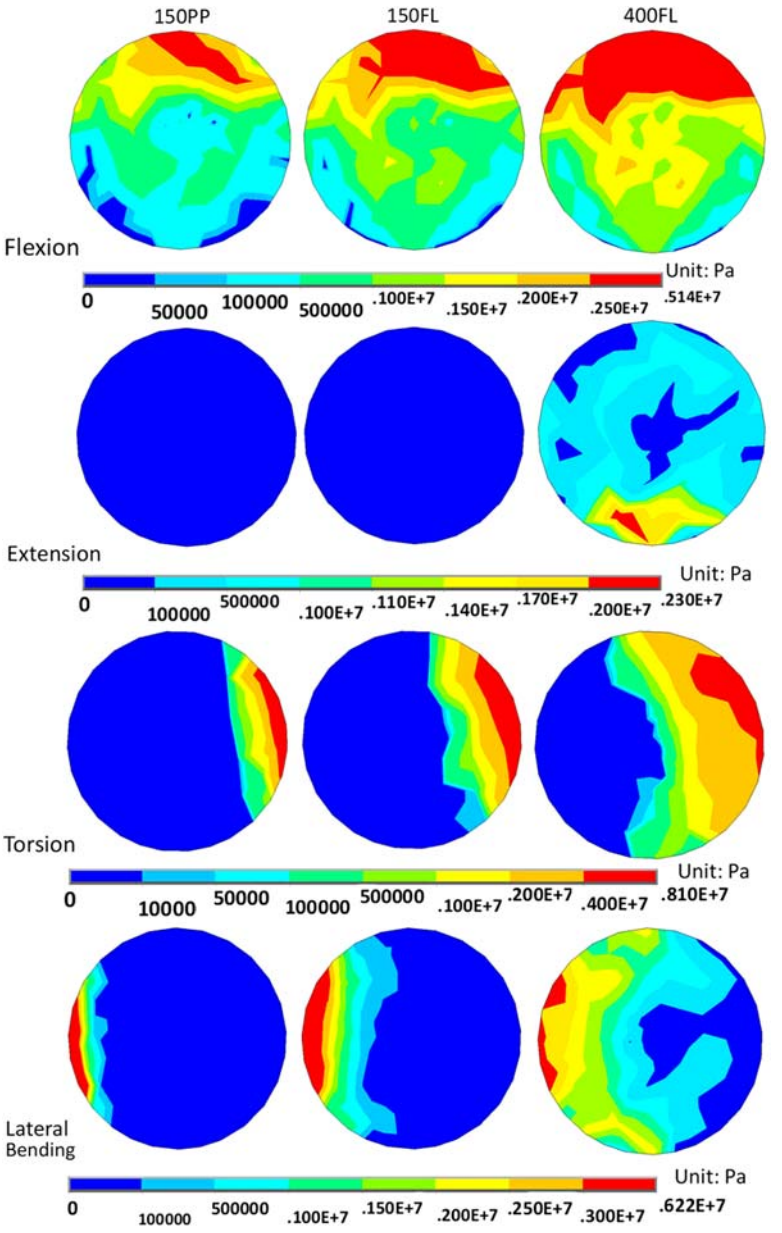

Figure 6. Contact pressure distribution pattern of the polyethylene inlay is shown for flexion (top), extension, torsion and lateral bending (bottom) under a PP of 150 N (left), FL of 150 N and FL of 400 N (right).

In addition, Punt et al. (2008) indicated that many patients require one or more reoperations due to facet hypertrophy after implantation of an artificial disc. In our simulations, the FCF gradually increased and reached 45% at the implanted level in torsion following the use of FL and increasing FL magnitudes. This finding implies that facet hypertrophy at the implanted level may be related to torsional motion under a patient's body weight. However, many factors, such as physiological changes that occur in the facet joint and the genetic disposition, and daily activity of the patient, were not considered in this study. Therefore, the clinical study and biomechanical research need to be confirmed in a future study.

In contrast to total disc replacement, clinical findings have indicated that facet hypertrophy develops noticeably at adjacent levels after spinal fusion (Lee 1988; Etebar and Cahill 1999). This study shows that FCF was clearly increased in extension and torsion regardless of the preload application method and magnitude. Although an FL of 400 N clearly decreased FCF by 27% in extension compared with a PP (148% vs. 121%), the FCF was still much higher than the intact value. Therefore, this study demonstrates that facet hypertrophy at adjacent segments may be related to

extension and torsion motions. In addition, the preload application method and magnitude would not affect the predictions for FCF in a fusion construct.

A recent prospective study has reported that disc replacement patients (8%) experienced a statistically lower rate of long-term adjacent-segment degenerative disease than fusion patients (20.9%; Guyer et al. 2009). Figure 5 shows that stress concentrated at the adjacent disc was more clearly observed in the ALIF model and that the stress distribution resembled the intact case in the ADR model, regardless of whether pressure or follower preload was used. This trend is in agreement with clinical findings (Park et al. 2004; Guyer et al. 2009). Therefore, this study demonstrated that different preload application methods or magnitudes would have no effect on the predicted trend in adjacent disc stress. In addition, this study found that the region in which stress was concentrated changed under different preloads. The presence of regions of concentrated stress at motion sites (such as the anterior region) might be related to adjacent disc degeneration; however, the stress concentration at the posterior region observed under a PP might have been induced by artefactual moments and forces.

This study has several limitations, including the fact that we did not consider various grades of disc degeneration. A degenerative disc would lead to a higher ROM, FCF and annular stress than would a healthy disc (Rohlmann et al. 2006). In addition, the role of the trunk muscles in generating FL was only identified for the intact lumbar spine and was simply assumed for both the spinal fusion and the total disc replacement cases. Finally, some deviations are still present in our results due to the difficulty of maintaining an ideal FL path while changing the posture.

Conclusions

This study found that the preload application method and magnitude affect the biomechanical behaviour of the lumbar spine. For the ADR, there was remarkable alteration while increasing the FL magnitude, particularly in the ROM, FCF and ICP. A higher FL of 400 N may be a better choice for biomechanical analysis of ADR. However, for the ALIF, the PP and FL method under the same load did not show any remarkable changes in terms of the ROM and adjacent disc stress.

References

Cappozzo A. 1984. Compressive loads in the lumbar vertebral column during normal level walking. J Orthop Res. 1:292–301.

Chen SH, Zhong ZC, Chen CS, Chen WJ, Hung C. 2009. Biomechanical comparison between lumbar disc arthroplasty and fusion. Med Eng Phys. 31:244–253.

Crisco JJ, Panjabi MM, Yamamoto I, Oxland TR. 1992. Euler stability of the human ligamentous lumbar spine. Part II: experiment. Clin Biomech. 7:27–32.

Etebar S, Cahill DW. 1999. Risk fractures for adjacent segment failure following lumbar fixation with rigid instrumentation for degenerative instability. J Neurosurg. 90:163–169.

Godest AC, Beaugonin M, Haug E, Taylor M, Gregson PJ. 2002. Simulation of a knee joint replacement during a gait cycle using explicit finite element analysis. J Biomech. 35: 267–275.

Goel VK, Grauer JN, Patel T, Biyani A, Sairyo K, Vishnubhotla S, Matyas A, Cowgill I, Shaw M, Long R et al., 2005. Effects of charite artificial disc on the implanted and adjacent spinal segments mechanics using a hybrid testing protocol. Spine. 30:2755–2769.

Guyer RD, McAfee PC, Banco RJ, Bitan FD, Cappuccino A, Geisler FH, Hochschuler SH, Holt RT, Jenis LG, Majd ME, et al., 2009. Prospective, randomized, multicenter food and drug administration investigational device exemption study of lumbar total disc replacement with the CHARITE artificial disc versus lumbar fusion: five-year follow-up. Spine J. 9: 374–386.

Kim K, Kim YH. 2008. Role of trunk muscles in generating follower load in the lumbar spine of neutral standing posture. J Biomech Eng. 130:0410051–0410057.

Kim K, Kim YH, Lee S. 2007. Increase of load-carrying capacity under follower load generated by trunk muscles in lumbar spine. Proc Inst Mech Eng Part H: J Eng Med. 221:229–235.

Lee CK. 1988. Accelerated degeneration of the segment adjacent to a lumbar fusion. Spine. 13:375–377.

Lemaire JP, Carrier H, Sariali el-H, Skalli W, F. 2005. Clinical and radiological outcomes with the Charite artificial disc: a 10-year minimum follow-up. J Spinal Disord Tech. 18: 353–359.

Liu CL, Zhong ZC, Hsu HW, Shih SL, Wang ST, Hung C, Chen CS. 2011. Effect of the cord pretension of the Dynesys dynamic stabilisation system on the biomechanics of the lumbar spine: a finite element analysis. Eur Spine J. 20:1850–1858.

Lu YM, Hutton WC, Gharpuray VM. 1996. Do bending, twisting, and diurnal fluid changes in the disc affect the propensity to prolapsed? A viscoelastic finite element model. Spine. 21: 2570–2579.

O'Leary P, Nicolakis M, Lorenz MA, Voronov LI, Zindrick MR, Ghanayem A, Havey RM, Carandang G, Sartori M, Gaitanis IN, et al., 2005. Response of charité total disc replacement under physiologic loads: prosthesis component motion patterns. Spine J. 5:590–599.

Panagiotacopulos ND, Pope MH, Krag MH, Krag MH. 1987. Water content in human intervertebral discs. Part I. Measurements by magnetic resonance imaging. Spine. 12:912–917.

Park P, Garton HJ, Gala VC, Hoff JT, McGillicuddy JE. 2004. Adjacent segment disease after lumbar or lumbosacral fusion: review of the literature. Spine. 29:1938–1944.

Patwardhan AG, Carandang G, Ghanayem AJ, Havey RM, Cunningham B, Voronov LI, Phillips FM. 2003a. Compressive preload improves the stability of anterior lumbar interbody fusion cage constructions. J Bone Joint Surg Am. 85:1749–1756.

Patwardhan AG, Havey RM, Carandang G, Simonds J, Voronov LI, Ghanayem AJ, Meade KP, Gavin TM, Paxinos O. 2003b. Effect of compressive follower preload on the flexion-extension response of the human lumbar spine. J Orthop Res. 21:540–546.

Patwardhan AG, Havey RM, Meade KP, Lee B, Dunlap B. 1999. A follower load increases the load-carrying capacity of the lumbar spine in compression. Spine. 24:1003–1009.

Patwardhan AG, Meade KP, Lee B. 2001. A frontal plane model of the lumbar spine subjected to a follower load: implications for the role of muscles. J Biomech Eng. 123:212–217.

Phillips FM, Cunningham B, Carandang G, Ghanayem AJ, Voronov L, Havey RM, Patwardhan AG. 2004. Effects of supplemental translaminar facet screw fixation on the stability of stand-alone anterior lumbar interbody fusion cages under physiologic compressive preloads. Spine. 29: 1731–1736.

Polikeit A, Ferguson SJ, Nolte LP, Orr TE. 2003. Factors influencing stresses in the lumbar spine after the insertion of intervertebral cages: finite element analysis. Eur Spine J. 12: 413–420.

Punt IM, Visser VM, van Rhijn LW, Kurtz SM, Antonis J, Schurink GW, van Ooij A. 2008. Complications and reoperations of the SB Charité lumbar disc prosthesis: experience in 75 patients. Eur Spine J. 17:36–43.

Renner SM, Natarajan RN, Patwardhan AG, Havey RM, Voronov LI, Guo BY, Andersson GB, An HS. 2007. Novel model to analyze the effect of a large compressive follower pre-load on range of motions in a lumbar spine. J Biomech. 40:1326–1332.

Rohlmann A, Neller S, Claes L, Bergmann G, Wilke HJ. 2001. Influence of a follower load on intradiscal pressure and intersegmental rotation of the lumbar spine. Spine. 26: E557–E561.

Rohlamnn A, Zander T, Rao M, Bergmann G. 2009a. Realistic loading conditions for upper body bending. J Biomech. 42: 884–890.

Rohlamnn A, Zander T, Rao M, Bergmann G. 2009b. Applying a follower load delivers realistic results for simulating standing. J Biomech. 42:1520–1526.

Rohlmann A, Zander T, Schmidt H, Wilke HJ, Bergmann G. 2006. Analysis of the influence of disc degeneration on the mechanical behaviour of a motion segment using the finite element method. J Biomech. 39:2484–2490.

Shim CS, Lee SH, Shin HD, Kang HS, Choi WC, Jung B, Choi G, Ahn Y, Lee S, Lee HY. 2007. CHARITE Versus ProDisc: a comparative study of a minimum 3-year follow-up. Spine. 32:1012–1018.

Shirazi-Adl A, Ahmed AM, Shrivastava SC. 1986. Mechanical response of a lumbar motion segment in axial torque alone and combined with compression. Spine. 11:914–927.

Tzermiadianos MN, Mekhail A, Voronov LI, Zook J, Havey RM, Renner SM, Carandang G, Abjornson C, Patwardhan AG. 2008. Enhancing the stability of anterior lumbar interbody fusion 2008. A biomechanical comparison of anterior plate versus posterior transpedicular instrumentation. Spine. 33: E38–E43.

van Ooij A, Cumhur Oner F, Verbout ABJ. 2003. Complications of artificial disc replacement: a report of 27 patients with the SB Charite' disc. J Spinal Disord Tech. 16:369–383.

Yamamoto I, Panjabi MM, Crisco T, Oxland T. 1989. Three-dimension movement of the whole lumbar spine and lumbosacral joint. Spine. 14:1256–1260.

Zhong ZC, Chen SH, Hung C. 2009. Load- and displacement-controlled finite element analyses on fusion and non-fusion spinal implants. Proc Inst Mech Eng Part H: J Eng in Med. 223:143–157.